

Harmonics generation in electron-ion collisions in a short laser pulse

H. Haberland

Institut für Physik, Universität Greifswald, Domstraße 10a, 17487 Greifswald, Germany

M. Bonitz and D. Kremp

Fachbereich Physik, Universität Rostock, Universitätsplatz 3, D-18051 Rostock, Germany

(Received 30 March 2001; published 18 July 2001)

Anomalously high generation efficiency of coherent higher field harmonics in collisions between *oppositely charged particles* in the field of femtosecond lasers is predicted. This is based on rigorous numerical solutions of a quantum kinetic equation for dense laser plasmas that overcomes limitations of previous investigations.

DOI: 10.1103/PhysRevE.64.0264XX

PACS number(s): 52.25.Dg, 05.30.-d, 52.38.-r

Modern high-intensity short-pulse lasers [1] have made it possible to create dense correlated plasmas under laboratory conditions promising a large variety of applications, e.g., [2,3]. Remarkable progress has been made in the field of time-resolved plasma diagnostics [4], interesting high-field phenomena have been observed, including production of multi-keV electrons and the generation of higher field harmonics [bremsstrahlung (BS)] in neutral gases. On the other hand, despite early predictions [5], harmonics generation in an *ionized medium due to collisions of oppositely charged particles* in the field has not been observed experimentally [6]. The reason is the low electron-ion collision frequency ν_{ei} in a low-density equilibrium plasma [7]. In this paper we demonstrate a drastic, more than six orders of magnitude, efficiency increase for dense *nonequilibrium plasmas* excited by a *femtosecond laser pulse* that should make this fundamental effect observable experimentally. Moreover, we predict coherent harmonics pulses that may be significantly shorter than the pump pulse.

A full theoretical description of dense laser plasmas requires the selfconsistent treatment of (i) hydrodynamic mass and energy transport of electrons and heavy particles, (ii) collective (mean-field) phenomena, and (iii) elastic and inelastic carrier collisions in the presence of the field. In recent years there have been substantial advances in the theoretical description of the first two effects, see, e.g., [3,8,9] and [10–12], respectively. However, these treatments, usually being based on Vlasov, Fokker-Planck, or particle-in-cell simulations, either neglect collisions completely or study them in a strongly simplified manner. In particular, they neglect the field effect on the collision process. This may be justified for very strong fields where the electron oscillation (“quiver”) velocity $v_0 \equiv eE_0/(m_e\Omega)$ is much larger than the thermal velocity v_{th} , and the collision frequencies ν_{ee} and ν_{ei} are much below the oscillation frequency Ω of the field. However, for field intensities below 10^{15} W/cm² and/or high plasma density ($n > 10^{20}$ cm⁻³) and low temperature, collisions are the dominant factor in field-matter interaction at short times. At a later stage, due to hydrodynamic motion of electrons and ions, plasma heating and expansion, field effects will govern the plasma behavior, although collisional processes such as inverse bremsstrahlung, e.g., [13,5,9] or impact ionization/recombination remain important.

When this transition occurs and *what physical processes* take place at the *early stage* is not known until now—to answer these questions is the main goal of this paper. Our analysis reveals that during this initial stage the plasma has a strongly anisotropic and non-Maxwellian electron distribution function that develops bunches of fast electrons. As a result of electron-electron collisions, eventually, a monotonically decaying distribution is approached, but this thermalization takes about $t_{rel} \sim 50\text{--}100$ fs. Finally, the most interesting effect is that, under the strong nonequilibrium conditions at these short times, the generation of higher field harmonics in *e-i* collisions is strongly enhanced.

The analysis of the initial stage of laser-matter interaction requires a quantum kinetic equation that fully includes non-ideal plasma effects, the importance of which has been noted frequently, e.g. [8,12]. Such an equation has recently been derived [14] and has the form

$$\left\{ \frac{\partial}{\partial t} + e_a \mathbf{E}(t) \cdot \nabla_{\mathbf{k}} \right\} f_a(\mathbf{k}_a, t) = \sum_b I_{ab}(\mathbf{k}_a, t), \quad (1)$$

where for the initial period spatial homogeneity may be assumed. The collision integrals are given by

$$\begin{aligned} I_{ab}(\mathbf{k}_a, t) = & 2 \int \frac{d\mathbf{k}_b d\bar{\mathbf{k}}_a d\bar{\mathbf{k}}_b}{(2\pi\hbar)^6} |V_{ab}(\mathbf{q})|^2 \delta(\mathbf{k}_{ab} - \bar{\mathbf{k}}_{ab}) \\ & \times \int_{t_0}^t d\bar{t} \cos \left[\frac{\epsilon_{ab} - \bar{\epsilon}_{ab}}{\hbar} (t - \bar{t}) - \frac{\mathbf{q}}{\hbar} \cdot \mathbf{R}_{ab}(t, \bar{t}) \right] \\ & \times \{ \bar{f}_a \bar{f}_b [1 - f_a] [1 - f_b] - f_a f_b [1 - \bar{f}_a] \\ & \times [1 - \bar{f}_b] \} |_{\bar{t}}, \end{aligned} \quad (2)$$

where a, b label electrons and ions, and we denoted $\epsilon_{ab} \equiv \epsilon_a + \epsilon_b$, $\epsilon_a \equiv p_a^2/2m_a$, $\mathbf{k}_{ab} \equiv \mathbf{k}_a + \mathbf{k}_b$, and $\mathbf{q} \equiv \mathbf{k}_a - \bar{\mathbf{k}}_a$. V_{ab} is the Fourier transform of the screened Coulomb potential $V_{ab}(q) = 4\pi e_a e_b / [q^2 + \kappa(t)^2]$, [$\kappa(t)$ is the inverse *nonequilibrium* screening length]. This allows us to avoid any cutoff (Coulomb logarithm). We underline that the collision integral I_{ab} is exact (within the static weak-coupling limit). In particular, it permits a rigorous investigation of the short-time physics and, for long times $t \gg 2\pi/\omega_{pl}$ [ω_{pl}

$= (4\pi n e^2/m)^{1/2}$ is the plasma frequency] and zero field ($R_{ab} = 0$), it goes over to the familiar Landau collision integral $\int d\vec{t} \cos \dots \rightarrow \hbar \pi \delta(\epsilon_{ab} - \bar{\epsilon}_{ab})$. Moreover, this integral includes Pauli blocking (spin statistics) and it conserves the *total energy* (kinetic plus potential energy) which is important for dense nonideal plasmas.

Most importantly, the integral I_{ab} includes the *influence of a strong field on the collision process* of two particles of species a and b exactly, as well as the effect of a finite collision duration $\tau_{\text{coll}} = t_2 - t_1$ that is crucial for the results shown below. Indeed, during the time τ_{coll} , each of the colliding particles gains a certain momentum $\mathbf{Q}_a(t_1, t_2)$ in the field, and a pair of colliding (oppositely charged) particles is displaced by the field a distance $\mathbf{R}_{ab}(t_1, t_2)$. For a harmonic field, $\mathbf{E}(t) = \mathbf{E}_0 \cos \Omega t$,

$$\mathbf{Q}_a(t_1, t_2) = \frac{-e_a \mathbf{E}_0}{\Omega} (\sin \Omega t_1 - \sin \Omega t_2), \quad (3)$$

$$\begin{aligned} \mathbf{R}_{ab}(t_1, t_2) &= \left(\frac{e_a}{m_a} - \frac{e_b}{m_b} \right) \frac{\mathbf{E}_0}{\Omega^2} \\ &\times \{ \cos \Omega t_1 - \cos \Omega t_2 - \Omega(t_2 - t_1) \sin \Omega t_1 \}, \end{aligned} \quad (4)$$

and these effects are growing with increasing field strength. The momentum shift enters the arguments of the distribution functions in the collision integral (2), (time-dependent intracollisional field effect): $f_a \equiv f[\mathbf{k}_a + \mathbf{Q}_a(t, \bar{t}), \bar{t}]$; $\bar{f}_a \equiv f[\bar{\mathbf{k}}_a + \mathbf{Q}_a(t, \bar{t}), \bar{t}]$, whereas \mathbf{R}_{ab} modifies the energy balance of the two-particle collisions in a monochromatic field. Thus, the collision integral (2) selfconsistently includes nonlinear field effects, such as harmonics generation, emission (absorption) of laser photons during the two-particle scattering [(inverse) BS], and generalizes previous treatments of these phenomena, e.g., [5,9], to the case of arbitrary short times, nonequilibrium distributions, and modifications by dense plasma effects.

We expect the most interesting physics to occur in situations where the effects of collisions and of the field are of the same order: (i) when the field frequency Ω is in the range of the collision frequency ν_{ei} and the plasma frequency ω_{pl} and, (ii) when the field-induced particle velocities v_0 are of the same order as the thermal velocity v_{th} . Thus, considering as an example, a dense fully ionized hydrogen plasma in a monochromatic optical field of intermediate wavelength $\lambda = 500$ nm ($\Omega = 3.77$ fs $^{-1}$), the following parameter range is of interest for the simulations: densities 10^{20} cm $^{-3} \leq n \leq 10^{24}$ cm $^{-3}$, corresponding to a plasma frequency range 0.56 fs $^{-1} \leq \omega_{pl} \leq 56$ fs $^{-1}$, and an initial plasma temperature of 20 000 K that may increase up to almost 10^6 K within the first 50 fs of the relaxation. Correspondingly, for this case, field strengths of interest are 10^7 V/cm $\geq E_0 \geq 10^9$ V/cm. For stronger fields ($I > 10^{15}$ W/cm $^{-2}$) collisions will already be of minor importance.

The main difficulty in the numerical solution of Eqs. (1–4) is the non-Markovian (time-nonlocal) structure of the collision integral. Such quantum kinetic equations have re-

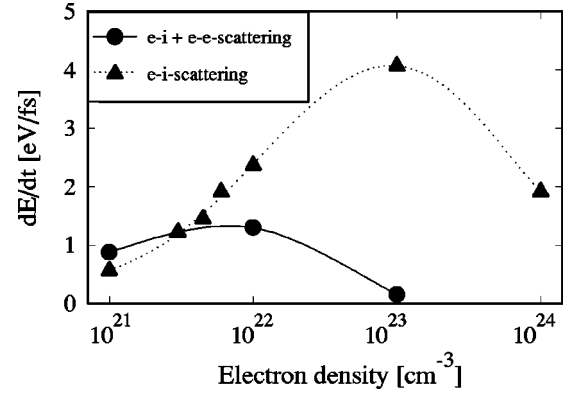


FIG. 1. Average electron kinetic energy increase per time versus density, with and without e - e scattering included. Field amplitude and wavelength are $E_0 = 3 \times 10^8$ V/cm and $\lambda = 500$ nm. The initial plasma temperature is $T_0 = 20\,000$ K.

cently been solved for an isotropic, e.g., [15], and anisotropic plasma [16], respectively. In contrast to these and other previous treatments, in the present paper, for the first time, the effect of a strong field on the collision process is fully included.

We solve Eqs. (1)–(4) by direct numerical integration starting from a pre-excited electron-ion plasma in equilibrium, and the relaxation is computed over about 50 field cycles. We underline that we solve Eqs. (1)–(4) without any simplifying assumptions. In particular, momentum anisotropy of the electron distribution function, as well as time and momentum retardation, are fully included. The ion distribution was found to remain a Maxwellian during the considered time interval that allowed us to simplify the integral I_{ei} . To properly account for the time dependence of the screened Coulomb potential $V(q)$, the inverse screening length $\kappa(t)$ is computed self consistently from the current nonequilibrium distribution functions. Solving the kinetic equation yields the time and momentum-dependent distribution function $f_e(\mathbf{k}, t)$ which allows us to compute all transport properties, including the mean electron kinetic energy density $\langle E_{\text{kin}}^e \rangle(t) = (m_e)/(2) \langle v_e^2 \rangle$ and the electrical current density $\mathbf{j}(t) = \sum_a e_a \langle \mathbf{v}_a \rangle$, [f is normalized to the density, and $\langle \dots \rangle$ denotes averaging over $f(t)$].

Let us now come to the results. First recall that, in the collisionless case ($I_{ab} = 0$), the electron distribution would oscillate as a whole according to $\sin \Omega t$ without changing shape. This yields no net current and no energy increase (the energy oscillates with 2Ω around the ponderomotive energy $U_{\text{pond}} = mv_0^2/4$). In contrast, in the presence of collisions, we observe a strong increase of the mean electron kinetic energy. After an initial transient of about 5 fs, $\langle E_{\text{kin}}^e \rangle$ grows almost linearly, thereby oscillating with 2Ω . This energy increase is due to *field-induced electron acceleration during electron-ion collisions*, cf. the term $\mathbf{q} \cdot \mathbf{R}_{ei}$ in the integral I_{ei} , Eq. (2). No net acceleration occurs in electron-electron collisions ($\mathbf{R}_{ee} = 0$). The energy growth rate depends on the ratio of field strength and density. This is shown in Fig. 1 where the average slope of the energy curves is plotted for different densities. Interestingly, the most efficient plasma

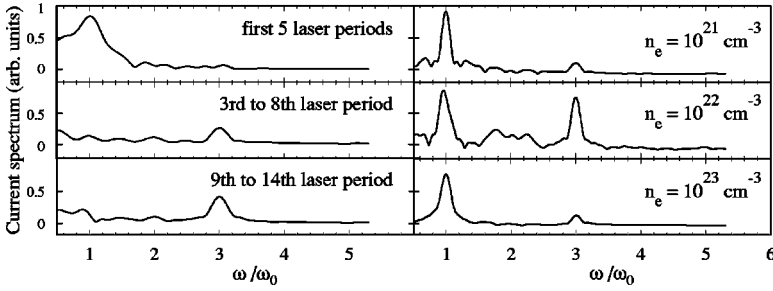


FIG. 2. Electrical current spectrum in a time-dependent electric field. The higher harmonics are the sole result of electron-ion collisions. Left column—time evolution of the spectrum for $n = 10^{22} \text{ cm}^{-3}$, from averaging over five laser periods at different moments (see text in this figure). Right column—spectrum (from averaging over the full calculation) for various densities. Other parameters are the same as in Fig. 1.

heating occurs around 10^{22} cm^{-3} , which is near the critical density $n_{cr} = 4.5 \cdot 10^{21} \text{ cm}^{-3}$, where $\omega_{pl} = \Omega$. The maximum value of the power is about 1.5 eV/fs, which roughly corresponds to the absorption of one photon per electron and laser cycle. Notice also that, although $e-e$ scattering does not contribute to the heating directly, this process may not be neglected, as this would lead to an overestimate of the power by a factor of 3 and a shift of the maximum to higher densities by one order of magnitude, cf. the triangles in Fig. 1.

Next, we consider the electrical current density. In contrast to the collisionless case, where $\mathbf{j}_0(t) = en\mathbf{v}_0 \sin \Omega t$, collisions between electrons and ions may give rise to higher field harmonics. Indeed, electrons oscillating with the field are disturbed by the Coulomb field of ions that yields a change of the electron velocity component in field direction ($v_0 \gg v_{th}$)

$$\Delta v_z(t) \approx \frac{a \sqrt{2}}{\Omega (1+b^2)} \frac{\sin \Omega t}{\sqrt{1+2b^2+\cos 2\Omega t}}, \quad (5)$$

$$\text{with } a = \frac{e_e e_i}{\mu r_0^2}, \quad b = \sqrt{\frac{r_\perp}{r_0}}, \quad r_0 = \left(\frac{e_e}{m_e} - \frac{e_i}{m_i} \right) \frac{E_0}{\Omega^2},$$

where $\mu^{-1} = m_e^{-1} + m_i^{-1}$, and r_\perp is the minimal electron-ion distance. One readily checks that in the spectrum of Eq. (5) appear all harmonics of the field. Formula (5) indicates that the spectrum will be particularly broad for close encounters (small r_\perp , strong scattering). Further, the efficiency of harmonics generation decreases with growing field strength. On the other hand, for the case of a weak field [not covered by Eq. (5)], the harmonics yield increases with E_0 (with the number of photons), resulting in a maximum of the efficiency around $v_0 = v_{th}$ [7,17]. Quantitative estimates for the conversion efficiency η_N (intensity of the N th harmonics normalized to the intensity of the fundamental oscillation) can be given for the case of Maxwellian electrons. Then, only odd harmonics exist and $\eta_N^{EQ} \sim (\nu_{ei}/\Omega)^2 / N^{\alpha_N}$, where $\alpha_N = \alpha_N(v_0/v_{th}) > 0$ [7]. Direct evaluation of the collision integral I_{ei} , Eq. (2), for a dense equilibrium plasma revealed that the highest value in equilibrium is $\eta_3^{EQ} \sim 10^{-7}$ [17].

However, as we show now, the efficiency may be increased drastically under nonequilibrium conditions of femtosecond laser pulse excitation. Figure 2 shows the results for the current spectrum obtained from the numerical solution of the quantum kinetic equations (1,2) for $E_0 = 3 \times 10^8 \text{ V/cm}$ and an initial temperature $T = 20\,000 \text{ K}$. Figure 2(a) shows the result for a density of $n = 10^{22} \text{ cm}^{-3}$ at dif-

ferent times (obtained by Fourier transforming $\mathbf{j}(t)$ over time intervals of five laser periods). One clearly sees the formation of strong third harmonics, which is comparable to and may even exceed the fundamental component, i.e., $\eta_3 \sim 1$. At later times, this peak vanishes again. We mention that higher odd harmonics are found for higher field strength also, besides, there is a clear signature of the second harmonics, cf. Fig. 2. The temporal behavior of the harmonics emission can be understood from the time evolution of the nonequilibrium cycle-averaged collision frequency

$$\nu_{ei}(E_0, \Omega; n, t) = 4\pi \frac{\Omega^2 \overline{\mathbf{j}(t) \cdot \mathbf{E}(t)}}{\omega_{pl}^2 \overline{\mathbf{E}^2(t)}}, \quad (6)$$

which is shown in Fig. 3. Due to the laser heating of the plasma, cf. Fig. 1, and relaxation towards a Maxwellian, the collision frequency ν_{ei} decreases in time, limiting the efficiency $\eta_N(t)$ and, thus, the duration of the harmonics pulse.

Finally, to understand the reason for the anomalously high efficiency of harmonics generation, we consider in Fig. 4 the temporal evolution of the electron distribution. The upper, middle, and lower figure parts show snapshots of $f_e(k_x, k_z)$ after 0, 6, and 12 complete field cycles, respectively. Clearly, the distribution is becoming anisotropic already during the first few laser periods. It strongly deviates from a Maxwellian, developing side peaks along the field direction, the dis-

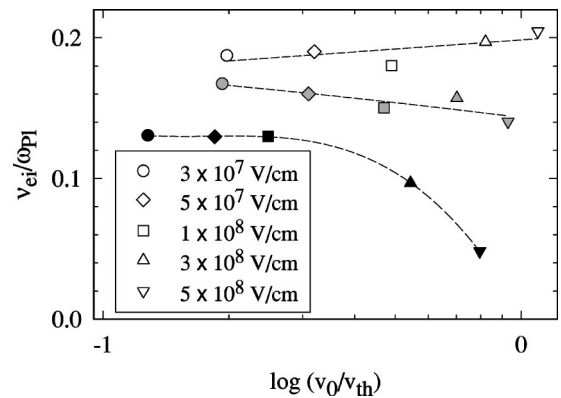


FIG. 3. Nonequilibrium collision frequency, Eq. (6), vs logarithm base 10 of the quiver velocity, at the initial moment, after 9 fs and after 25 fs (white, gray, and black symbols, respectively). $n = 10^{22} \text{ cm}^{-3}$, $v_{th} \equiv \sqrt{\langle v_e^2 \rangle}$. Due to collisional energy absorption, cf. Fig. 1, during the relaxation, symbols move to the left. Symbols with same shape refer to the same field strength, lines are guides to the eye.

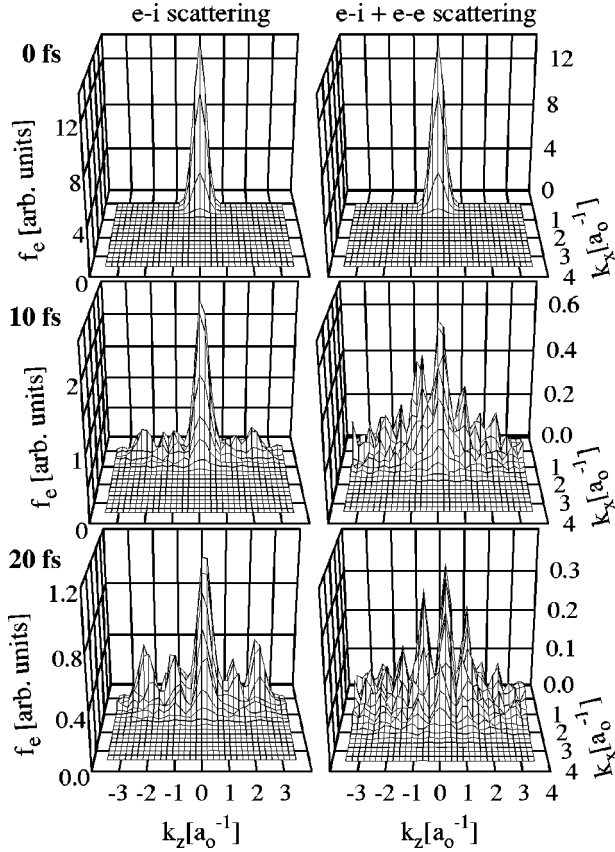


FIG. 4. Evolution of the electron distribution function in momentum space (the field is in the k_z direction) with only electron-ion collisions included (left column) and with electron-ion and electron-electron collisions (right column), respectively. Figure shows snapshots at $t=0$ (upper figures), after 6 laser periods (middle) and after 12 laser periods (bottom), when the main peak of f_e is at the origin (the distribution as a whole oscillates with the field in k_z direction and is isotropic in the k_x - k_y plane). Note the different vertical scales.

tance of which from the origin is proportional to the field strength. This peculiar nonequilibrium behavior is caused by electron-ion collisions in the presence of the field, as can be seen from the left column, where electron-electron collisions are neglected. These features are observed for all considered densities and field strengths (see above), but they are strongest around $\Omega = \omega_{pl}$ and $v_0 = v_{th}$. Under these conditions, an electron spends the maximum possible time in the field of an ion (extending over approximately $r_D = \kappa^{-1}$) per laser cycle, $\Omega \tau_{coll} \sim \Omega r_D / v_{th} \sim \Omega / \omega_{pl} \sim 1$. These are the optimal condi-

tions for collisional e-i momentum exchange in the field, as for electron acceleration (inverse BS), cf. Fig. 1, and harmonics emission (BS), Fig. 2(b).

Our calculations show that, as a result of $e-e$ collisions (right column of Fig. 4), the side peaks of f_e are formed more rapidly, and they are squeezed towards the center. After 30–50 fs the peaks start to smear out, and after $t_{rel} \sim 50$ –100 fs (depending on the density) a monotonically decaying distribution with a temperature of the order of several 10^6 K is reached. By this time the plasma has become essentially collisionless: ν_{ei} has decayed to its equilibrium value [18] and $\nu_{ee} \approx 0$, making it necessary to include collective and hydrodynamic (spatial heat flow, expansion, etc.) effects, as mentioned in the Introduction, while for the treatment of collisions simpler models may be used.

In summary, we have presented a self-consistent numerical investigation of the early relaxation stage, $t \leq 50$ fs, of a preionized dense plasma in a laser field with $E_0 = 10^7$ – 10^9 V/cm. We have found the formation of a strongly nonequilibrium electron distribution giving rise to coherent bremsstrahlung emission of ultrashort third-harmonics pulses. An anomalously high conversion efficiency (more than six orders of magnitude compared to plasmas in equilibrium) is predicted, which should make this fundamental process accessible for experimental observation. To reduce limiting factors such as phase matching requirements, as well as competing effects (e.g., resonantly generated harmonics near the critical density profile), the experiments should use a very thin foil, e.g. [4], and work with a weakly undercritical plasma. The most favorable conditions are expected for a preionized plasma with high charge state since ($\nu_{ei} \sim Z$) excited by a linearly polarized laser pulse with a duration τ_p shorter than 50 fs where the third harmonics should be observable in transmission. To further improve the quantitative predictions, the plasma generation process has to be included in the simulation. For example, ionization from excited atomic levels should enhance the harmonics yield [7], accelerate the plasma heating, and thus, further reduce the duration of the higher-harmonics pulse. Finally, we mention that our results are not limited to laser plasmas, but are equally important for electron-hole plasmas subject to intense THz radiation.

This work is supported by the Deutsche Forschungsgemeinschaft (Schwerpunkt ‘‘Laserfelder’’), the European Commission through the TMR Network SILASI, and the NIC Jülich. We acknowledge stimulating discussions with R. Sauerbrey, M. Schlanges, and V.P. Silin.

- [1] For a recent overview, see, e.g., M.D. Perry and G. Mourou, *Science* **264**, 917 (1994).
 [2] M. Tabak *et al.*, *Phys. Plasmas* **1**, 1626 (1994).
 [3] E.G. Gamaliy, *Laser Part. Beams* **12**, 185 (1994).
 [4] W. Theobald, R. Hässner, C. Wülker, and R. Sauerbrey, *Phys. Rev. Lett.* **77**, 298 (1996).
 [5] V.P. Silin, *Zh. Éksp. Teor. Fiz.* **47**, 2254 (1964) [*Sov. Phys.*

JETP **20**, 1510 (1964)].

- [6] The BS mechanism is fundamentally different from the collisionless harmonics generation in relativistic plasmas, see, e.g., P. Gibbon, *IEEE J. Quantum Electron.* **33**, 1915 (1997), and references therein.
 [7] See V.P. Silin, *Zh. Éksp. Teor. Fiz.* **117**, 926 (2000) [*Sov. Phys. JETP* **90**, 805 (2000)]; *Kvant. Elektron. (Moscow)* **26**, 11

- (1999).
- [8] W. Rozmus and V.T. Tikhonchuk, Phys. Rev. A **42**, 7401 (1990).
- [9] For a recent overview and further references, see D. Vick, C.E. Capjack, V. Tikhonchuk, and W. Rozmus, Comments Plasma Phys. Control. Fusion **17**, 87 (1996).
- [10] H. Ruhl *et al.*, Phys. Rev. Lett. **82**, 743 (1999).
- [11] A. Pukhov and J. Meyer-ter-Vehn, Phys. Rev. Lett. **76**, 3975 (1996).
- [12] H. Ruhl *et al.*, Phys. Rev. Lett. **82**, 2095 (1999).
- [13] J. Dawson and C. Oberman, Phys. Fluids **5**, 517 (1962).
- [14] D. Kremp, Th. Bornath, M. Bonitz, and M. Schlages, Phys. Rev. E **60**, 4725 (1999).
- [15] M. Bonitz *et al.*, J. Phys.: Condens. Matter **8**, 6057 (1996); N. Kwong and M. Bonitz, Phys. Rev. Lett. **84**, 1768 (2000).
- [16] R. Binder, H.S. Köhler, M. Bonitz, and N. Kwong, Phys. Rev. B **55**, 5110 (1997).
- [17] P. Hilse (unpublished).
- [18] Th. Bornath, M. Schlages, P. Hilse, D. Kremp, and M. Bonitz, Laser Part. Beams **18**, 535 (2000).